

Optical properties of the iron-pnictide analog BaMn_2As_2

A. Antal,^{1,2} T. Knoblauch,¹ Y. Singh,³ P. Gegenwart,³ D. Wu,^{1,*} and M. Dressel¹

¹*Physikalisches Institut, Universität Stuttgart, Pfaffenwaldring 57, 70550 Stuttgart, Germany*

²*Institute of Physics, Budapest University of Technology and Economics and Condensed Matter Research Group, Hungarian Academy of Sciences, 1521 Budapest, Hungary*

³*Physikalisches Institut, Georg-August-Universität Göttingen, 37077 Göttingen, Germany*

(Dated: July 11, 2012)

We have investigated the infrared and Raman optical properties of BaMn_2As_2 in the ab -plane and along the c -axis. The most prominent features in the infrared spectra are the E_u and A_{2u} phonon modes which show clear TO-LO splitting from the energy loss function analysis. All the phonon features we observed in infrared and Raman spectra are consistent with the calculated values. Compared to the iron-pnictide analog AFe_2As_2 , this compound is much more two-dimensional in its electronic properties. For $E \parallel c$ -axis, the overall infrared reflectivity is insulating like. Within the ab -plane the material exhibits a semiconducting behavior. An energy gap $2\Delta=48$ meV can be clearly identified below room temperature.

PACS numbers: 74.25.Gz, 74.70.Xa, 74.25.Jb, 74.20.Rp

I. INTRODUCTION

The discovery of superconductivity in layered $\text{LaFeAsO}_{0.9}\text{F}_{0.1}$ four years ago has brought a new trend to synthesize and study new materials which are analogous to this compound.^{1,2} By now, most of the interest is focussed on the materials as AM_2X_2 “122”-type, AFeX “111”-type and FeX “11”-type which have high superconducting transition temperature T_c and can be obtained as high-quality single crystals. Only few studies have been reported on low T_c pnictide compounds or those that do not show superconductivity at all.²⁻⁵ Among those is BaMn_2As_2 , that has the same tetragonal ThCr_2Si_2 -type structure as MFe_2As_2 at room temperature and undergoes no structural transition upon cooling.⁵ The antiferromagnetic order appears at $T_N = 625$ K; i.e. at much higher temperature than for the MFe_2As_2 compounds.⁶ While most of the AM_2X_2 parent compounds are metallic, BaMn_2As_2 is a semiconductor with a small band gap $\Delta \approx 27$ meV according to dc -resistivity measurement.⁵ An *et al.* suggested that the difference in magnetic and electronic properties compared to those of MFe_2As_2 is due to the strong Hund’s coupling, the stability of the half-filled d -shell of the Mn^{2+} (d^5 ion) and strong spin-dependent Mn-As hybridization.⁷

In this paper, we present mainly the infrared studies on BaMn_2As_2 single crystals with the electric field polarized within the ab -plane and parallel to the c -axis. The sample with a size of $5 \times 5 \times 1$ mm³ was grown out of Sn fluxes. The magnetic, transport, and thermal properties of our material have been reported recently.^{5,6} For the infrared reflectance measurements, we cleaved the crystal within the ab -plane and finely polished the ac -plane in order to get shiny surfaces. The temperature dependent reflectivity spectra were measured in a wide frequency range from 40 to 37 000 cm⁻¹ using Fourier-transform infrared spectrometers (40 – 15 000 cm⁻¹) and a variable-angle spectroscopic ellipsometer (6000 – 37 000 cm⁻¹, restricted to

room temperature). Raman spectra were measured using Jobin-Yvon T64000 spectrometer equipped with a microscope at room temperature. We used 514.5 nm Ar-laser excitation line with intensity below 1 mW. Spectra were measured in (a,a) and (b,b) polarizations. Several infrared and Raman phonon modes are assigned and compared to the calculated values.

II. EXPERIMENTAL RESULT AND DISCUSSION

In the inset of Fig. 1, we plot the room temperature reflectivity for both ab -plane and c -axis polarization in the entire measured frequency range (40 to 37 000 cm⁻¹). As approaching the zero frequency, R_{ab} shows an up-turn towards unity reflectance while R_c tends to keep a constant value of approximately 40%. The rather low overall reflectivity ($\sim 30\%$) indicates that BaMn_2As_2 is a rather bad metal or a semiconductor. Besides the pronounced phonon vibrations in far-infrared region which we will discuss in detail later in this paper, two interband transition can be identified at approximately 7000 cm⁻¹ (0.87 eV) and 26 000 cm⁻¹ (3.2 eV).^{8,9} The temperature dependence of the reflectivity spectra is displayed in Fig. 1(a) and (b). In the ab -plane, the reflectivity below 700 cm⁻¹ increases with decreasing temperature, indicating a metallic behavior. This is consistent with the dc -resistivity measurement reported in Ref. 5. Only a very small temperature dependence is observed along the c -axis due to the less conducting property.

A. Phonon vibrations

Due to the low reflection and weak absorption of BaMn_2As_2 in the ab -polarization, a small fraction (about 5%) of the far-mid infrared light was found to be transmitted through the sample during the quality-check mea-

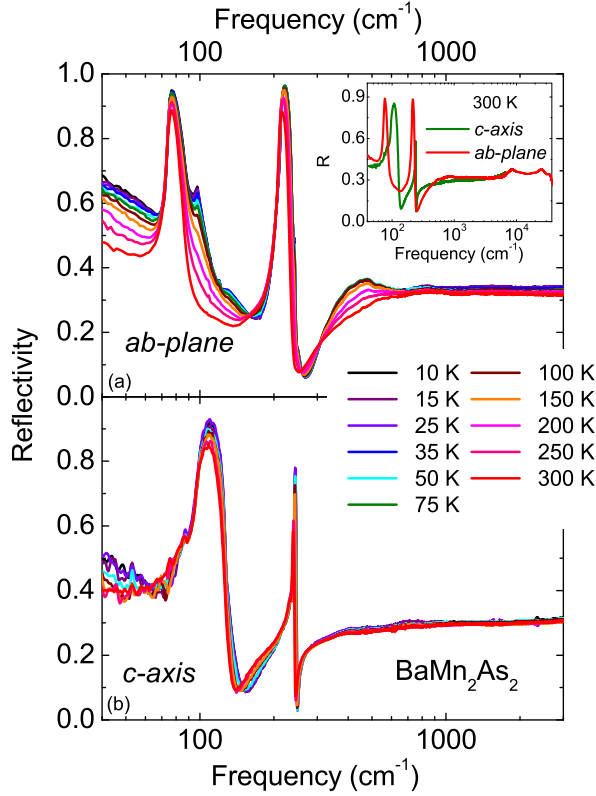


FIG. 1: (Color online) Temperature dependent optical reflectivity of BaMn_2As_2 measured in (a) the ab -plane and (b) along the c -direction. The inset shows the room-temperature reflectivity in the whole measured range ($40 - 37\,000\text{ cm}^{-1}$).

TABLE I: Comparison of the phonon mode frequencies (in cm^{-1}) found in different AM_2X_2 compounds with the resonance frequencies of BaMn_2As_2 .

Mode	CaFe_2As_2	SrFe_2As_2	BaFe_2As_2	EuFe_2As_2	BaMn_2As_2
A_{1g}	189	182			174
B_{1g}	211	204	209		
E_g		114	124		
E_g		264	264		
A_{2u}					96/131
A_{2u}					230/243
E_u			94		74/92
E_u			253, 254	260	210/238
Ref.	12	13	14-16	8	this work

surement. This prevents us from a correct evaluation of conductivity spectra as commonly done by a Kramers-Kronig analysis.¹⁰ Nevertheless, all the pronounced phonon vibration modes show Lorentzian like shapes and thus are applicable for extracting the physics behind. According to the tetragonal ThCr_2Si_2 -type structure (with space group $I4/mmm$) in which the

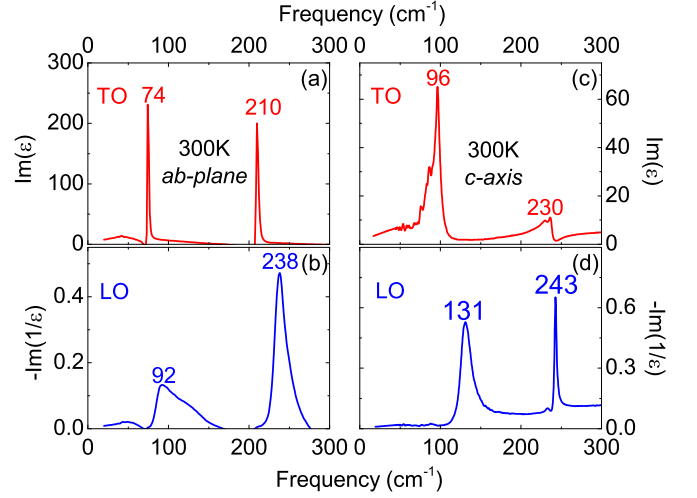


FIG. 2: (Color online) Imaginary part of the dielectric function $\text{Im}(\epsilon)$ and $-\text{Im}(1/\epsilon)$ at 300 K for BaMn_2As_2 single crystal with (a,b) $E||ab$ and (c,d) $E||c$. The frequencies of transverse optical (TO) and longitudinal optical (LO) modes are respectively identified as labeled in each panel.¹⁸

AM_2X_2 usually crystallizes, a group theoretical analysis of the phonon modes in BaMn_2As_2 yields $A_{1g} + B_{1g} + 2E_g$ Raman-active, $2A_{2u} + 2E_u$ infrared-active and $A_{2u} + E_u$ acoustic optical zone center phonons, where A/B and E modes correspond to an atomic motion perpendicular and parallel to MnAs planes, respectively.^{11,13} In our infrared spectra, however interestingly, we observe at least four vibration modes both in ab -plane and along the c -axis, as shown in Fig. 1. Thus we extract the imaginary part of the dielectric function $\text{Im}(\epsilon)$ and $-\text{Im}(1/\epsilon)$ (known as the energy loss function) to identify the possible split transverse optical (TO) and longitudinal optical (LO) modes, respectively.¹⁷ According to Fig. 2, we can directly label the TO/LO energies to be 74/92 cm^{-1} and 210/238 cm^{-1} for two E_u modes, 96/131 cm^{-1} and 230/243 cm^{-1} for two A_{2u} modes.

In Fig. 3 we show a room-temperature XX (A_{1g} and B_{1g} modes are allowed) Raman spectrum of BaMn_2As_2 as obtained in (a,a) and (b,b) polarizations. A pronounced peak can be observed at 174 cm^{-1} . We refer this contribution to the A_{1g} mode which is corresponding to the As-As displacement along c -axis (see also in Fig. 4).

In Table.I a comparison of phonon modes frequencies found in BaMn_2As_2 and several AFe_2As_2 ($A=\text{Ca, Ba, Sr and Eu}$) compounds is shown. Due to the differences in lattice constant, atomic mass, and possible magnetic interactions (especially for EuFe_2As_2 and BaMn_2As_2), the vibration frequencies for the same phonon mode are slightly different in these materials.

To compare with theoretical values, we also carried out phonon calculations (in the *nonmagnetic* state (NM)) on the density-functional perturbation theory level within the plane-wave method with the generalized gradient approximation (GGA) of Perdew-Burke-Enzerhof.^{19,20} We

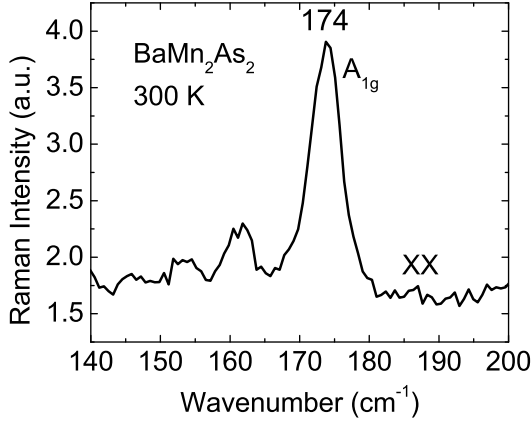


FIG. 3: (Color online) XX-polarized Raman spectrum of BaMn_2As_2 at 300 K. The peak at 174 cm^{-1} is assigned as A_{1g} mode.

used the quantum espresso package for the electronic structure calculation with the implemented ultrasoft plane-wave basis set.²¹ The band occupation was fixed and the literature lattice parameters has been used.²² Only the atomic positions in the unit cell were optimized. The Brillouin zone is sampled in the \mathbf{k} space with a uniform Monkhorst-Pack grid ($12 \times 12 \times 12$).²³ In Fig. 4, we display the calculated atomic transverse optical displacements and the measured TO/LO frequencies for all zone center phonons. Note that, in our calculations only a small LO-TO splitting of less than 1 cm^{-1} could be observed. The reason for such a small splitting and the discrepancy in the frequencies bases mainly on the non-magnetic state revealing no band gap. An et al.⁷ show by using density functional theory that the ground state of BaMn_2As_2 is antiferromagnetic (AFM) with a small bandgap of about 0.2 eV in the case of GGA calculations. Recent *ab initio* calculations of the phonon spectrum in the “122”-family including the magnetic interaction lead to a better agreement of the phonon spectrum.^{24–26} The difference in the mode frequencies between the NM and the AFM state can exceed 40 cm^{-1} .²⁷ It would be desirable to conduct further calculations including the AFM state which should lead to a small band gap and consequently a bigger LO-TO splitting.⁷

In Fig. 5, no change in the phonon shape is observed for these modes due to the absence of structural transition upon cooling. But the E_u mode with higher vibrational frequency is enhanced in intensity and continuously shift to higher frequencies. Recent neutron diffraction measurement on the thermal contraction revealed that by cooling from 300 K to 10 K, $d_{\text{Mn-As}}$ distance decrease from 2.566(2) to 2.558(2).⁶ The lattice distortion with reducing bond lengths enhances the electronic interactions between atoms and therefore the phonon vibrating energy increases – consistent with the observed blue shift of this E_u mode in our spectra.

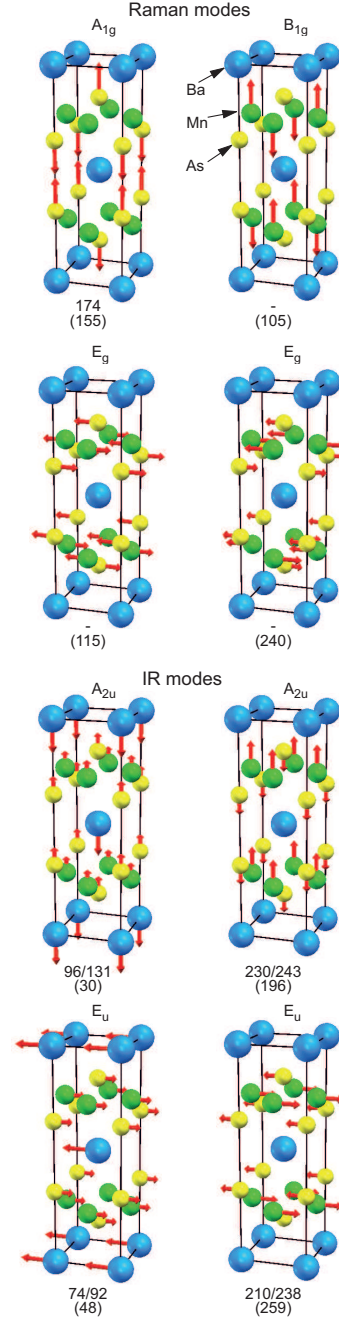


FIG. 4: (Color online) Calculated atomic displacements and TO/LO frequencies in cm^{-1} for zone center phonons. Calculated frequencies are shown in brackets.

B. Energy gap

There is an extra broad hump at the frequency around 400 cm^{-1} in the in-plane reflectivity spectra, as shown in Fig.1(a). According to the phonon calculations, we can exclude it to be a phonon mode. As the optical conductivity spectra of BaMn_2As_2 are phonon-rich ones, we will here analyze the optical data by looking at the relative change of the conductivity $\Delta\sigma_1(\omega, T) = \sigma_1(\omega, T) -$

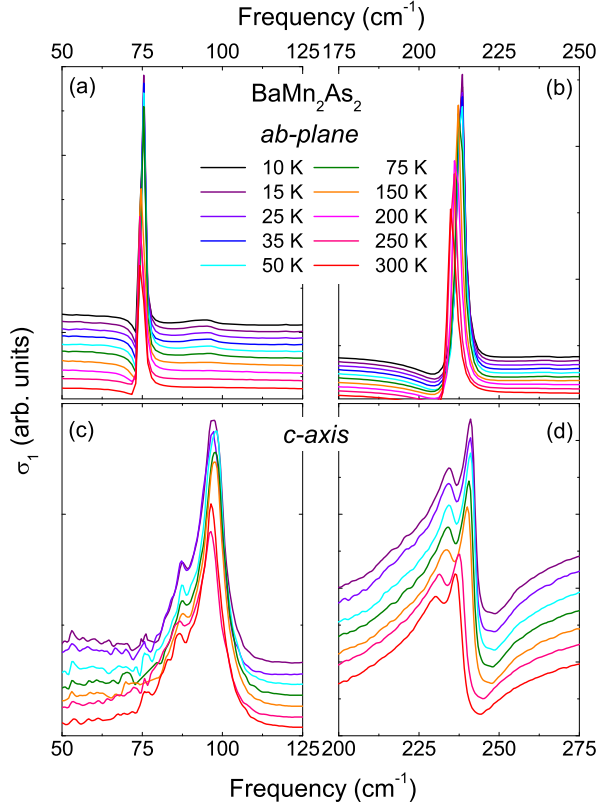


FIG. 5: (Color online) Temperature development of conductivity in the region of phonon modes of BaMn_2As_2 .

$\sigma_1(\omega, T_0 = 300 \text{ K})$, as plotted Fig. 6, to get rid of the strong phonon oscillations and see basically only the electronic background and consequently the spectral weight redistribution upon varying the temperature. As seen in Fig. 6, around 300 cm^{-1} $\Delta\sigma_1 = \sigma_1(\omega, T) - \sigma_1(\omega, 300 \text{ K})$ drops to negative values with decreasing temperature, then it increases at higher frequency and crosses zero at 440 cm^{-1} indicating that the spectral weight redistributes from low to high energies. Such a spectral weight rearrangement is the typical signature for an energy gap formation. From the minimum of $\Delta\sigma_1(10 \text{ K})$ we estimate the gap value $2\Delta \sim 390 \text{ cm}^{-1}$ (48 meV).^{8,28} Interestingly, Singh *et al.* recently performed a gap analysis on the *dc*-conductivity curve of this material.⁵ There two linear ranges were found in the $\ln\{\sigma(T)\}$, and according to the expression $\ln\{\sigma\} = A - \Delta/k_B T$ two activation energies $\Delta = 27 \text{ meV}$ and $\Delta = 6.5 \text{ meV}$ were derived respectively. The gap value we yield from our optical experiments is in accord with the bigger one.²⁹

C. Anisotropy

The *c*-axis conductivity (Fig. 7) varies only slightly with temperatures. When $\omega \rightarrow 0 \text{ cm}^{-1}$, no Drude like behavior is observed and $\sigma_1(\omega \rightarrow 0)$ is quite low, indicating that the material is insulating along the *c*-axis.

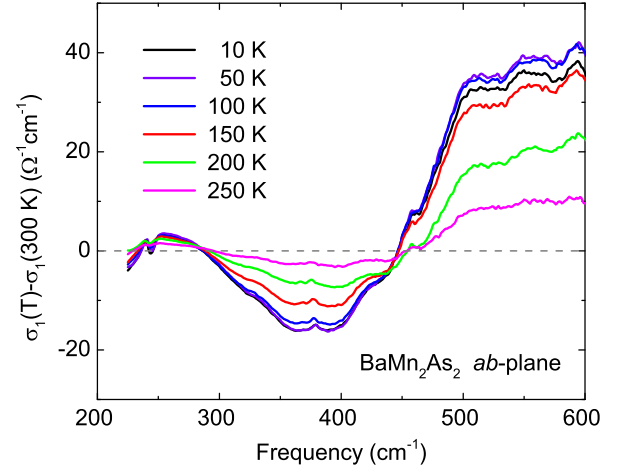


FIG. 6: (Color online) $\Delta\sigma_1(\omega, T) = \sigma_1(\omega, T) - \sigma_1(\omega, 300 \text{ K})$ at selected temperatures.

No transfer of spectral weight is induced by the gap opening. In contrast to iron-pnictides $M\text{Fe}_2\text{As}_2$, the present compound BaMn_2As_2 reveals distinctively different electronic properties for the in-plane and out-of-plane directions, i.e. the material is more two-dimensional. In previous optical studies on BaFe_2As_2 by Wang and collaborators,³⁰ the metallic responses were found for both $E \parallel ab$ and $E \parallel c$ with an anisotropy-factor about three.³¹ While two spin-density-wave gaps were revealed in the *ab*-plane, one of them also opens along the *c*-axis, giving evidence for a three-dimensional Fermi surface in the electronic structure.³⁰ Furthermore, the low carrier mobility in BaMn_2As_2 infers more localized charge carriers, in the contrast to the itinerant nature of the electronic properties of $M\text{Fe}_2\text{As}_2$. The reason is the antiferromagnetic arrangement of the Mn^{2+} spins both in the *ab*-plane and along the *c*-axis (G-type antiferromagnetic order), where at low temperature the electron hopping between nearest neighbor sites with opposite spin is suppressed and a strong scattering is induced by the spin disorder at high temperature.⁷

III. SUMMARY

In summary, the optical properties of iron-pnictide analog BaMn_2As_2 have been studied in detail using light polarized in the *ab*-plane and along the *c*-axis. Within the *ab*-plane, the material behaves like a poor metal or semiconductor. An energy gap can be defined at $2\Delta=48 \text{ meV}$. The *c*-axis spectra show a typical insulating behavior overall and no energy gap is found. This indicates that the BaMn_2As_2 is a two-dimensional electron system rather than a quasi three-dimensional, as the Fe-pnictides are considered to be. The E_u and A_{2u} phonon modes have clear TO/LO splitting with frequencies differences of $10\text{-}40 \text{ cm}^{-1}$. A systematic comparison between experimental results and theoretical calculations

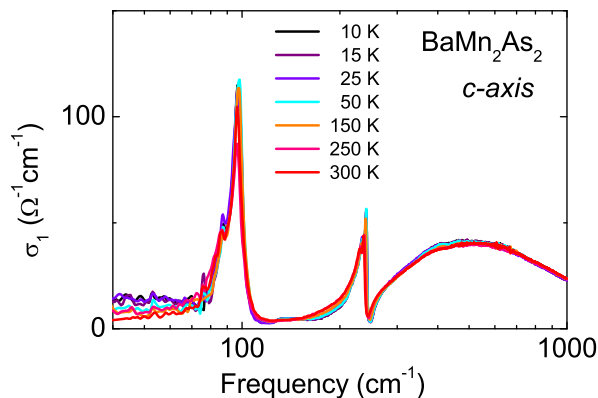


FIG. 7: (Color online) c -axis conductivity of BaMn_2As_2 as a function of frequency from 40 to 1000 cm^{-1} measured at selected temperatures.

are present for all the infrared and Raman modes.

Acknowledgments

We thank B. Gorshunov and V. I. Torgashev for very helpful discussions. We appreciate N. Drichko at Johns Hopkins University, Baltimore MD, for performing the Raman measurement. The contributions of J. Braun and D. Rausch to the experiments are appreciated. D.W acknowledges her fellowship by the Alexander von Humboldt Foundation. A.A. acknowledges the support of the German Academic Exchange Service (DAAD) and also Hungarian National Research Fund OTKA NN76727. T.K. acknowledges his scholarship by the Carl-Zeiss-Stiftung. Part of the work was funded by the Deutsche Forschungsgemeinschaft (DFG).

-
- * Electronic address: dan.wu@pi1.physik.uni-stuttgart.de
- ¹ Y. Kamihara, T. Watanabe, M. Hirano, and H. Hosono, *J. Am. Chem. Soc.* **130**, 3296 (2008).
 - ² D. C. Johnston, *Adv. Phys.* **59**, 803 (2010).
 - ³ F. Ronning, N. Kurita, E. D. Bauer, B. L. Scott, T. Park, T. Klimczuk, R. Movshovich, and J. D. Thompson, *J. Phys.: Condens. Matter* **20**, 3422033 (2008)
 - ⁴ R. Nath, V. O. Garlea, A. I. Goldman, D. C. Johnston, *Phys. Rev. B* **81**, 224513 (2010).
 - ⁵ Y. Singh, A. Ellern, and D. C. Johnston, *Phys. Rev. B* **79**, 094519 (2009).
 - ⁶ Y. Singh, M. A. Green, Q. Huang, A. Kreyssig, R. J. McQueeney, D. C. Johnston, and A. I. Goldman, *Phys. Rev. B* **80**, 100403 (2009)
 - ⁷ J. An, A. S. Sefat, D. J. Singh, and M.-H. Du, *Phys. Rev. B* **79**, 075120 (2009).
 - ⁸ D. Wu, N. Barišić, N. Drichko, S. Kaiser, A. Faridian, M. Dressel, S. Jiang, Z. Ren, L. J. Li, G. H. Cao, Z. A. Xu, H. S. Jeevan and P. Gegenwart, *Phys. Rev. B* **79**, 155103 (2009)
 - ⁹ G. Li, W. Z. Hu, J. Dong, Z. Li, P. Zheng, G. F. Chen, J. L. Luo, and N. L. Wang, *Phys. Rev. Lett.* **101**, 107004 (2008).
 - ¹⁰ M. Dressel and G. Grüner, *Electrodynamics of Solids* (Cambridge University Press, Cambridge, 2002).
 - ¹¹ E. Kroumova, M. I. Aroyo, J. M. Perez-Mato, A. Kirov, C. Capillas, S. Ivantchev and H. Wondratschek, *Phase Transition* **76**, 155-170 (2003).
 - ¹² K.-Y. Choi, D. Wulferding, P. Lemmens, N. Ni, S. L. Bud'ko and P. C. Canfield, *Phys. Rev. B* **78**, 212503 (2008).
 - ¹³ A. P. Litvinchuk, V. G. Hadjiev, M. N. Iliev, Bing Lv, A. M. Guloy and C. W. Chu, *Phys. Rev. B* **78**, 060503(R) (2008).
 - ¹⁴ L. Chauvière, Y. Gallais, M. Cazayous, A. Sacuto, M. A. Méasson, D. Colson and A. Forget, *Phys. Rev. B* **80**, 094504 (2009).
 - ¹⁵ A. Akrap, J. J. Tu, L. J. Li, G. H. Cao, Z. A. Xu, and C. C. Homes, *Phys. Rev. B* **80**, 180502 (2009).
 - ¹⁶ A. A. Schafgans, B.C. Pursley, A. d. LaForge, A. S. Sefat, D. Mandrus and D. N. Basov, *Phys. Rev. B* **84**, 052501 (2011).
 - ¹⁷ P.-Y. Yu and M. Cardona, *Fundamentals of Semiconductors, Physics and Materials Properties* (Springer, 1996).
 - ¹⁸ In Fig. 2(a) and (b), there are ranges (for example, 170-210 cm^{-1}) where $\text{Im}(\epsilon)$ shows negative values. This unphysical phenomenon is caused by the transparent property of sample as we discussed at the beginning of II-A section.
 - ¹⁹ S. Baroni, S. de Gironcoli, A. Dal Corso and P. Giannozzi, *Rev. Mod. Phys.* **73**, 515-560 (2001).
 - ²⁰ J. P. Perdew, K. Burke, and M. Enzerhof, *Phys. Rev. Lett.* **77**, 3865 (1996).
 - ²¹ P. Giannozzi *et al.*, *J. Phys.: Condens. Matter*, **21**, 395502, (2009).
 - ²² Y. Singh, M. A. Green, Q. Huang, A. Kreyssig, R. J. McQueeney, D. C. Johnston and A. I. Goldman *Phys. Rev. B* **80**, 100403 (2009).
 - ²³ H. J. Monkhorst and J. D. Pack, *Phys. Rev. B* **13**, 5188 (1976).
 - ²⁴ R. Mittal, S. Rols, M. Zibri, Y. Su, H. Schober, L. Chaplot, M. Johnson, M. Tegel, T. Chatterji, S. Matsuishi, H. Hosono, D. Johrendt and Th. Brueckel, *Phys. Rev. B* **79**, 144516 (2009).
 - ²⁵ M. Zbiri, H. Schober, M. R. Johnson, S. Rols, R. Mittal, Y. Su, M. Rotter and D. Johrendt, *Phys. Rev. B* **79**, 064511 (2009)
 - ²⁶ E. Aktürk and S. Ciraci, *Phys. Rev. B* **79**, 184523 (2009).
 - ²⁷ P. Kumar, A. Bera, D. V. S. Muthu, A. Kumar, U. V. Waghmare, L. Harnagea, C. Hess, S. Wurmehl, S. Singh, B. Böhner and A. K. Sood, *J. Phys.: Condens. Matter* **23** (2011) 255403.
 - ²⁸ W. Z. Hu, J. Dong, G. Li, Z. Li, P. Zheng, G. F. Chen, J. L. Luo and N. L. Wang, *Phys. Rev. Lett.* **101**, 257005 (2008).
 - ²⁹ At around 100 cm^{-1} we observed a similar but very small hump at 10 K and 50 K. It can be due to the formation of a smaller gap $2\Delta=12$ meV. As this gap-like feature only appears below 75 K, it should be referred to the second

gap $\Delta=6.5$ meV measured in *dc*-resistivity by Singh *et. al* in Ref.5.

³⁰ Z. G. Chen, T. Dong, R. H. Ruan, B. F. Hu, B. Cheng, W. Z. Hu, P. Zheng, Z. Fang, X. Dai, and N. L. Wang, Phys.

Rev. Lett. **105**, 097003 (2010).

³¹ In the case of EuFe_2As_2 the anisotropy was about a factor of 8 (Ref. 8).